Non-stoichiometric Relationship between Clathrin Heavy and Light Chains Revealed by Quantitative Comparative Proteomics of Clathrin-coated Vesicles from Brain and Liver*[S]

Martine Girard‡, Patrick D. Allaire, Peter S. McPherson§, and Francois Blondeau¶

We used tandem mass spectrometry with peptide counts to identify and to determine the relative levels of expression of abundant protein components of highly enriched clathrin-coated vesicles (CCVs) from rat liver. The stoichiometry of stable protein complexes including clathrin heavy chain and clathrin light chain dimers and adaptor protein (AP) heterotetramers was assessed. We detected a deficit of clathrin light chain compared with clathrin heavy chain in non-brain tissues, suggesting a level of regulation of clathrin cage formation specific to brain. The high ratio of AP-1 to AP-2 in liver CCVs is reversed compared with brain where there is more AP-2 than AP-1. Despite this, general endocytic cargo proteins were readily detected in liver but not in brain CCVs, consistent with the previous demonstration that a major function for brain CCVs is recycling synaptic vesicles. Finally we identified 21 CCV-associated proteins in liver not yet characterized in mammals. Our results further validate the peptide accounting approach, reveal new information on the properties of CCVs, and allow for the use of quantitative proteomics to compare abundant components of organelles under different experimental and pathological conditions. ***Molecular & Cellular Proteomics 4: 1145–1154, 2005.***

Vesicle budding and trafficking via clathrin-coated pits (CCPs)[1] and vesicles (CCVs) provides a major route by which proteins are transported out of the trans-Golgi network (TGN) and by which receptors, transporters, and nutrients are endocytosed at the plasma membrane (1–3). Many clathrin-dependent trafficking events mediate cargo transport that is needed in all cell types. These "housekeeping" forms of clathrin trafficking include the turnover of plasma membrane proteins and lipids, endocytic uptake of nutrients such as iron-saturated transferrin and low density lipoproteins, and endocytosis of a diverse range of activated growth factor receptors (1–3). Moreover all cells have housekeeping trafficking at the TGN. An important example is the delivery of mannose 6-phosphate-tagged lysosomal hydrolases from the TGN to endosomes/lysosomes via the mannose 6-phosphate receptor (MPR) (4).

In addition to these housekeeping activities of CCVs, some tissues have specialized trafficking needs. For example, in secretory cells, clathrin coats are involved in the formation of secretory granules at the TGN (5), and polarized cells utilize CCVs for the trafficking of certain receptors from the TGN to the basolateral membrane necessary for the maintenance of polarity (2). At the plasma membrane, intestinal epithelial cells in rat or placental cells in humans use CCVs for the uptake of maternal immunoglobulins, a necessary aspect of maternal derived immunity (6). A striking example of specialized CCV function is seen in neurons, which communicate by releasing neurotransmitters through fusion of synaptic vesicles with the plasma membrane following transient increases in Ca^{2+} concentration (7). These vesicles are then retrieved through CCVs (8–10). Thus, neurons need CCVs not only for housekeeping forms of clathrin-mediated endocytosis but also to retrieve synaptic vesicle membranes. It has been unclear whether or not the mechanisms mediating these two related but distinct events taking place at the plasma membrane could be distinguished. Moreover the relative amount of brain CCVs specialized for synaptic function has never been assessed.

The presence of clathrin adaptor proteins (APs) can provide one level of discrimination of vesicle type as CCVs arising from the TGN contain AP-1 and CCVs derived from the plasma membrane contain AP-2. AP-1 and AP-2 are heterotetramers composed of four subunits each, namely γ-, β_1-, μ_1-, and σ_1-adaptin for AP-1 and α-, β_2-, μ_2-, and σ_2-adaptin for AP-2 (11). Two genes code for α-adaptin giving rise to αA and αC variants with an alternative brain-specific splice form for αA (12). AP-1 and AP-2 provide a link between membranes and clathrin, the major component of CCVs (13). In addition, AP-2 stimulates clathrin assembly, whereas this as-

From the Department of Neurology and Neurosurgery, Montreal Neurological Institute, McGill University, Montreal, Québec H3A 2B4, Canada

Received, February 14, 2005, and in revised form, June 2, 2005
Published, MCP Papers in Press, June 2, 2005, DOI 10.1074/mcp.M500043-MCP200

[1] The abbreviations used are: CCP, clathrin-coated pit; AP, adaptor protein; CHC, clathrin heavy chain; CLC, clathrin light chain; CCV, clathrin-coated vesicle; EM, electron microscopy; FENS-1, FYVE domain-containing protein localized to endosomes 1; GRASP, Golgi peripheral membrane protein p65; MPR, mannose 6-phosphate receptor; NECAP 1, adaptin-ear-binding coat-associated protein 1; RME-8, receptor-mediated endocytosis 8; TGN, trans-Golgi network.

sembly activity is significantly reduced for AP-1 (14). The reduced clathrin assembly activity of AP-1 at the TGN may be taken up by other proteins such as enthoprotin (15). Clathrin itself is composed of heterodimers of clathrin heavy chain (CHC) and one of two clathrin light chains (CLCs), CLCa and CLCb. CHC/CLC dimers form a structure referred to as a triskelia that has been shown in CCVs derived from brain to be composed of three CHCs and three CLCs (16, 17). The 1:1 stoichiometry of CHC to CLC in brain CCVs has been confirmed by quantitative proteomics (18). This notion regarding the structure of clathrin triskelia has been extended to all tissues without further testing and has gradually become dogmatic.

To better understand the structure and function of CCVs, we have taken advantage of an approach that we recently developed to determine the relative levels of proteins within complex mixtures using tandem MS (18). The approach works on the principle that the more abundant a protein is, the more peptides it will generate upon trypsin digest. These peptides will be sampled more often in the mass spectrometer, thus giving more spectra. Of course this will depend on the length of the protein as longer proteins will generate more peptides and also on the amino acid composition of the protein as certain peptides will be more readily resolved and detected than others. Regardless, differences in peptide numbers between proteins within a sample should provide a reflection of their relative ratios. Indeed we have been able to demonstrate the molar ratios of abundant components of CCVs from rat brain (18). The approach was independently demonstrated by Liu *et al.* (19) who spiked complex protein mixtures with known concentrations of test proteins. They determined that changes in the number of MS/MS spectra identified for a given protein correlated directly to changes in its concentration over several orders of magnitude (19). In this study, we performed a proteomic analysis of highly purified CCVs from rat liver. Application of the peptide accounting approach, when compared with a similar analysis on brain CCVs, allowed us to reveal new information regarding the machinery for CCV formation.

EXPERIMENTAL PROCEDURES

Antibodies—Monoclonal antibodies for CHC, AP-1 (γ-adaptin), and AP-2 (α-adaptin) were from BD Biosciences. Monoclonal antibody CON.1, which recognizes CLCa and CLCb, was from Santa Cruz Biotechnology. Monoclonal antibody X16 against CLCa (20) was a generous gift of Dr. Frances Brodsky.

Preparation and Analysis of Liver CCVs—Liver CCVs were isolated using procedures described previously (21, 22) from adult rats that had been starved overnight. Suspensions of liver CCVs were deposited on 0.22-μm nitrocellulose filters to ensure random sampling (23) and were then processed for electron microscopy (EM) using an osmium tetroxide and tannic acid double fixation procedure (24). The purity of liver CCVs was assessed by counting the number of coated vesicles and contaminants in pictures taken from randomly selected fields from six independent preparations.

Liver CCV proteins were separated by SDS-PAGE, and each lane was cut into 66 slices (Supplemental Fig. 1). Each slice was individually processed for tandem MS as described previously (18). Spectra were analyzed by MASCOT software to identify tryptic peptide sequences matched to the National Center for Biotechnology Information (NCBI) non-redundant protein database with a confidence level of 95% or greater (25). Specific and shared peptides with an equal or greater score than the identity score were kept and recorded for each band. Peptides from the entire lane were then grouped based on their GI number and thus defined as specific peptides for their cognate protein. To add another level of confidence, only proteins found in two of three preparations and with five or more peptides were retained (26).

Other Subcellular Fractionation Procedures—CCVs were isolated from adult rat brains as described previously (15, 22). For specific experiments, CCVs were isolated from the livers of starved adult rats using the same protocol. For analysis on velocity gradients, ~1 mg of liver or brain CCVs isolated using this protocol was layered on linear 20–50% sucrose gradients prepared in buffer A (100 mM MES, pH 6.5, 1 mM EGTA, 0.5 mM $MgCl_2$) and centrifuged in a Sorvall AH629 rotor at 145,000 $\times$ *g* for 1.5 h. The gradients were fractionated from the bottom, and proteins from equal volume aliquots of each fraction were analyzed by SDS-PAGE and Western blot. To prepare P2 microsomes, various tissues and cell lines were homogenized in buffer A as described previously (22). The samples were centrifuged at 17,000 $\times$ *g* for 20 min, and the supernatant was further centrifuged at 56,000 $\times$ *g* for 1 h. Variable amounts of protein from the resulting microsomal (P2) fractions from each tissue were analyzed by SDS-PAGE and Western blot to generate an equivalent signal for the CHC. The supernatant (cytosolic fraction, S2) was also analyzed by Western blot. In other cases, microsomal fractions were prepared from 1 g each of two different tissues mixed together prior to homogenization or from 2 g of a single tissue. For these samples, gels were loaded with 100 μg of microsomes prepared from a single tissue and 200 μg of mixed tissues to account for the dilution of the tissues when mixed together.

RESULTS

Isolation of CCVs—CCVs were isolated from the livers of starved, adult rats using a well establish protocol (21, 22). Enrichment for protein bands corresponding to the molecular masses of CHC, CLCs, and the α-, β-, γ- and μ-adaptin subunits of the AP-1 and AP-2 complexes was observed in the consecutive fractions of the CCV preparation (Fig. 1*A*). The enrichment of CHC, CLCs, and γ-adaptin was demonstrated by Western blot (Fig. 1*B*). Transmission EM on the most highly enriched CCV preparation (P5, Fig. 1*A*) using filtration methods to ensure a random sampling of the material (22, 23) revealed the presence of CCVs recognizable based on their basket-like shape (Fig. 1*C*). Uncoated and partially coated vesicles heterogeneous in shape and size were also seen. Quantitation of the number of CCVs compared with various contaminants in 95 randomly selected fields from six independent preparations demonstrated that the CCVs were 89.3% pure (see Fig. 1*C* for a typical view of a randomly sampled EM field).

Protein Identification by Tandem MS—The proteins from three independent CCV preparations were separated on 5–16% gradient SDS-PAGE gels and cut into 66 even, horizontal slices (Supplemental Fig. 1). Each slice was processed for trypsin in-gel digest followed by LC Q-TOF MS/MS. To minimize the number of false positives, only proteins in which

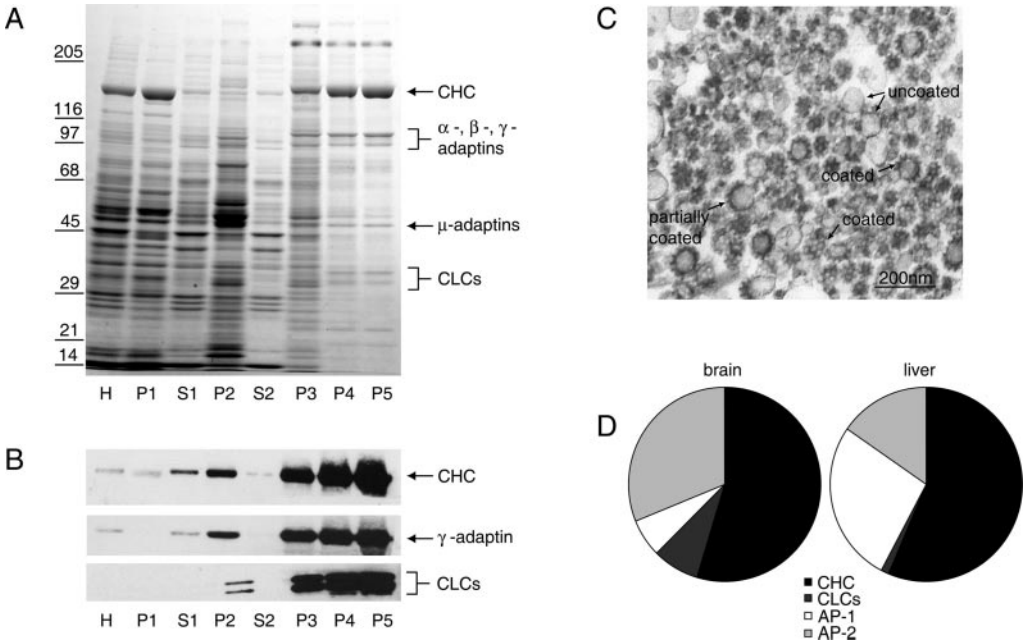

FIG. 1. **Isolation and characterization of liver CCVs.** *A*, Coomassie blue staining of proteins separated by SDS-PAGE from each step of the enrichment protocol for CCVs. Aliquots of 40 μg of protein were loaded on each lane. *H*, homogenate; *P*, pellet; *S*, supernatant. The predicted migratory positions of CHC, CLCs, and α-, β-, γ- and μ-adaptins are indicated. *B*, protein fractions from each step of the enrichment protocol for CCVs were processed for Western blot with CHC, CLC, and γ-adaptin (AP-1) antibodies. *C*, CCV fractions were evaluated by random sampling EM. A representative field is shown and reveals examples of coated, uncoated, and partially coated CCVs. *Bar*, 200 nm. *D*, pie chart representation of the proteomic results showing total number of peptides for all three preparations of liver CCVs and previously analyzed brain CCVs (18) for CHC, CLCs, and all of the subunits of the AP-1 and AP-2 complexes.

MS/MS spectra (identified with a 95% or greater confidence, see "Experimental Procedures") were found in at least two of the three replicates with at least five peptides in total were retained. All identified proteins were searched against each other by BLAST to ensure that all redundant identifications were collapsed into a single entry. Because of the high degree of homology between different tubulin isoforms, all tubulins were placed into one of two groups, tubulin α and β. With these criteria, we reproducibly identified 346 proteins in the liver CCV preparations including 21 novel proteins (Table I and supplemental table). As expected, all known CCV coat proteins were identified with multiple peptides (supplemental table). Interestingly the total number of peptides for CHC and CLCs and the sum of the total number of peptides for the subunits of AP-1 and AP-2 from liver (Fig. 1*D*, *right*) showed a distinct pattern from that seen in brain (Fig. 1*D*, *left*). Specifically for a comparable portion of CHC, the level of CLCs was reduced in liver compared with brain (Fig. 1*D*). Also the ratio of AP-1 to AP-2 was distinct in the two tissues with a high AP-1 to AP-2 ratio in liver and a much lower ratio in brain (Fig. 1*D*).

Ratio of CHC to CLC—When adjusted for protein size, peptide counts provide a very good measure of the relative abundance of proteins in complex mixtures (18). When applied to CHC and the total amount of both CLCa and CLCb, the peptide:mass ratio revealed that there are fewer CLCs than CHC in liver CCVs (3.13 peptides/kDa for CHC and 0.65 peptides/kDa for CLCs; Fig. 2*A*). This is surprising because it is generally thought that CHC and CLCs form as stable heterodimers leading to a 1:1 ratio in all tissues, and peptide accounting on brain CCVs did indeed reveal a 1:1 molar ratio for the proteins (Fig. 2*A*) (18). Consistent with peptide counts, Western blot analysis with a pan-CLC antibody showed that for a comparable CHC signal there is less signal for CLCs in CCVs from liver than CCVs from brain (Fig. 2*B*). CLCs from brain possess additional exons making them migrate more slowly on SDS-PAGE gels (27, 28). However, the CLC antibody recognizes an epitope that is conserved between the different splice forms of both CLCa and CLCb that are found in different tissues. Moreover because we apportioned the number of peptides to the size of the protein, differences in size would not affect the comparison between CHC and CLCs by peptide counts.

The protocol used to isolate liver CCVs for MS analysis, based on that of Pilch *et al.* (21), was different from that used for isolation of CCVs from brain, which was based on the protocol of Maycox *et al.* (29). This was due to the fact that the later protocol yielded CCVs that were ~50% pure when applied to liver tissue (data not shown). However, the deficit in the ratio of CLCs to CHC determined by Western blot in liver CCVs compared with brain CCVs was comparable when the CCVs were prepared in parallel using the Maycox *et al.* (29) protocol for each tissue (Fig. 3 and data not shown). Thus, the change in the ratio of CHC to CLCs was not due to different isolation procedures.

TABLE I
Novel proteins found in liver CCVs

NECAP 1, enthoprotin, and FENS-1 are in bold to indicate their previous identification as novel proteins in the proteome of brain CCVs (15). ARF, ADP-ribosylation factor.

	Protein name	Mass	Total peptides	NCBI GI nos.				
		Da						
1	**NECAP 1**	**37,228**	**8**	**37945074**	**27229051**	**27713302**	**15079260**	
2	**Enthoprotin; epsin 4**	**68,273**	**319**	**7661968**	**13278582**	**20345123**	**21751443**	**26006105**
3	RIKEN cDNA 6030446I19 gene	112,066	7	31542027	13449265	24980923		
4	RIKEN cDNA 5730596K20, homology to ARF-like 6-interacting protein 2	60,993	12	16877810	26326645	31559920	10435296	13477255
5	Similar to hypothetical protein MGC12103 (*Homo sapiens*)	46,194	5	27679620	27532965			
6	Similar to hypothetical protein KIAA0678 (RME-8)	306,705	59	27721389	26006199	28546047	26328693	26350527
7	KIAA0255 gene product	73,235	6	7662028	26352305	31542095	26339180	
8	KIAA0183	116,963	8	1136426	3005744	8922114	16307515	28524994
9	Similar to KIAA1414 protein	226,839	16	27478091	26348058			
10	Similar to mKIAA0219 protein	316,133	6	27666086				
11	**FENS-1**	**47,904**	**5**	**18482373**	**7243268**	**19484187**	**30795186**	
12	Unknown (*H. sapiens*)	24,209	17	3005742	12857585	12857927	18490304	20531765
13	Hypothetical protein D10Wsu52e	55,631	15	21703842	6841456	7657015	7688673	21703842
14	Similar to protein transport protein Sec24C (SEC24-related protein C)	112,455	6	27673609	20072091	27722283	28477301	28916673
15	EH domain-containing 4	60,888	16	10181214	7212811	7657056	10181214	20302075
16	Similar to Vault poly(ADP-ribose) polymerase (VPARP)	126,096	28	28479540				
17	Similar to ATP-binding cassette, subfamily A (ABC1), member 6	65,888	18	27690422	34875258			
18	Dendritic cell protein GA17	42,946	21	21703762	23397429	27702767	3152660	12751096
19	Similar to deleted in polyposis 1-like 1	39,229	7	27717621				
20	Macrophage expressed gene 1	74,478	5	12018298	2137564	18676680	20482397	
21	Vacuole 14 protein; Vac14 protein; hydin	89,095	5	29293817	26327751	26338430	31542488	

We next examined the relative ratio of CHC to CLCs in microsomal preparations. This allowed us to compare multiple tissues and to minimize sample handling times to reduce any potential influence of tissue-specific proteolysis of CLCs. For a comparable signal of CHC, normalized to that found in the brain, each tissue examined exhibited a deficit of CLCs compared with brain (Fig. 2*C*). Moreover for a comparable signal of CHC, CLCs were variably less abundant in five separate cell lines with the ratio in COS-7 cells closest to that seen in the brain (Fig. 2*D*). A deficit in CLCs relative to CHC was also seen in crude lysates prepared from the cell lines compared with crude brain homogenate (Supplemental Fig. 2). To further rule out a potential influence of proteolysis, we performed Western blots with monoclonal antibody X16, which is specific to CLCa but is strong on Western blot and is thus capable of detecting CLCa fragments. Even on long exposures, no lower molecular weight fragments were seen in microsomes prepared from multiple tissues with the exception of those from kidney, which demonstrated extensive proteolysis (Supplemental Fig. 3). Interestingly proteolysis of CLCa was also seen in liver and brain when those tissues were mixed with kidney tissue prior to preparation of microsomes but was not observed upon mixing liver and brain with any other tissues (Supplemental Fig. 3). Thus, the seeming lack of CLCs in kidney microsomes (Fig. 2*C*) appears to result from proteolysis, although proteolysis appears unlikely to account for the reduction of CLCs seen in other non-brain tissues. Our results support the notion that CLCs and CHC are not obligate heterodimers in liver and other non-brain tissues.

It is possible that the deficit in CLCs relative to CHC in liver CCVs occurs specifically on a single population of CCVs, that is, AP-1-positive CCVs from TGN/endosomes or AP-2-positive CCVs from the plasma membrane. Alternatively the deficit may be seen on both CCV populations. To examine this issue, we isolated liver and brain CCVs and subjected them to sedimentation on linear sucrose velocity gradients. In liver, AP-2 (α-adaptin)-containing CCVs peak one fraction closer to the bottom of the gradient than AP-1 (γ-adaptin)-containing CCVs, suggesting that, in this tissue, AP-2-positive CCVs are slightly larger (Fig. 3). CHC and CLCs appear to co-distribute throughout the gradient, suggesting that the ratio of the two proteins is equivalent at both the AP-1 and AP-2 vesicle peaks (Fig. 3). Thus, there does not appear to be a selective enrichment of CHC relative to CLCs on a specific population of CCVs. Notably the clathrin proteins peak with the AP-1-positive CCVs, which represent the major population of CCVs in liver (see below). In brain, AP-1-positive CCVs migrate deeper

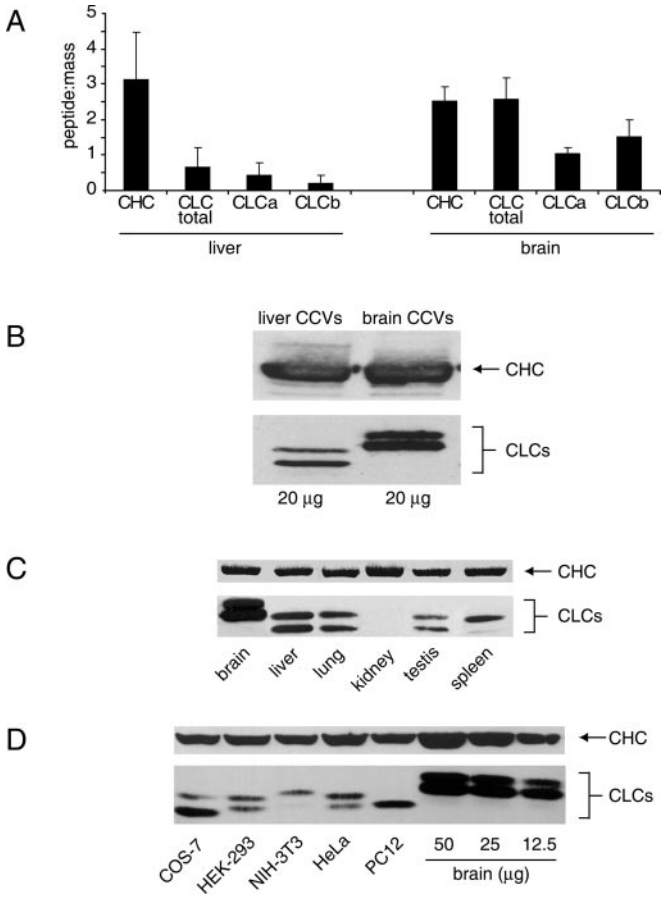

FIG. 2. **Ratio of CHC to CLCs.** *A*, the total number of peptides found in each preparation of liver and brain CCVs for CHC, CLCa, and CLCb was divided by the calculated mass of each protein (in kilodaltons) giving a peptide:mass ratio. The *bars* and *error bars* represent the mean and S.E. between the three preparations for each tissue. *B*, aliquots of liver and brain CCVs (20 µg for each) were processed for Western blot with antibodies against CHC and CLCs. *C*, crude microsomal fractions were prepared from different tissues and processed for Western blot with antibodies against CHC and CLCs. Variable amounts of protein were loaded to obtain an equal signal for the CHC. *D*, crude microsomal fractions were prepared from different cell lines and processed for Western blot with antibodies against CHC and CLCs. Variable amounts of protein from each cell line were loaded to obtain an equal signal for the CHC. Different concentrations of brain microsomes were loaded as indicated. *HEK*, human embryonic kidney.

into the gradients than AP-2-positive CCVs (Fig. 3, note that the AP-2 blot was deliberately underexposed to emphasize the distribution of the protein on the gradient). CHC and CLCs co-migrate on the gradient as expected given that the ratio of the proteins is 1:1 in brain (Fig. 3).

Ratio of AP-1 to AP-2—AP-2 is a marker of plasma membrane-derived CCVs and in brain was found in a 5:1 molar excess to the TGN/endosome adaptor AP-1 (18). In contrast, by averaging the subunit counts for each adaptor complex as was done for brain (18), we demonstrated an overall 2:1 excess of AP-1 to AP-2 in liver CCVs (Fig. 4*A*). This inversion of the AP-1 to AP-2 ratio was due to both an increase in the relative amount of AP-1 and a decrease in the relative amount of AP-2 in liver compared with brain (Fig. 4*A*). Interestingly the decrease in AP-2 in liver appears to be accounted for primarily by a decrease in the αA isoform, whereas the αC isoform is present in liver and brain at comparable levels (Fig. 4*B*). The ratio of total AP complexes to total CHC from liver is the same as in brain; namely CCVs from both tissues exhibit the same deficit of APs to CHC (Fig. 4*A*).

The observations on the ratios of the AP complexes between CCVs from brain and liver determined by peptide counts were supported by Western blot. Indeed the γ-adaptin signal was stronger for CCVs from liver than for CCVs from brain, whereas an α-adaptin antibody specific for the αA isoform revealed the opposite pattern (Fig. 4*A*, *inset*). αA from brain and muscle contains an additional 21-amino acid insert that is responsible for the apparent size change of αA between brain and liver (12), although the epitope for the antibody is conserved between the splice variants. A stronger signal for AP-1 γ-adaptin in liver than brain relative to a comparable amount of CHC was also seen when CCVs were generated from the two tissues using the same protocol (Fig. 3). The seeming decrease in AP-2 α-adaptin in brain relative to liver CCVs in Fig. 3 was due to the low exposure of the blot, and in fact when the α-adaptin blots from the two tissue samples were exposed for the same time, the AP-2 signal was stronger in the brain than in the liver samples (data not shown). The bias toward AP-1-positive CCVs in liver is also in agreement with the detection of a larger amount of TGN cargo such as the cation-independent and cation-dependent MPRs in liver than in brain CCVs (Fig. 4*C*).

Determination of the Percentage of CCVs in Brain Specialized for Synaptic Vesicle Recycling—The relative ratio of CCVs between the TGN/endosome and the plasma membrane that is used for generalized housekeeping forms of membrane trafficking should be similar in most tissues. We thus calculated the number of AP-2-positive CCVs in brain that would come from non-specialized forms of CCV traffic based on the ratio between AP-1 and AP-2 found in liver. In liver, AP-1- and AP-2-positive CCVs represented 65.4 and 34.6%, respectively, of the total number of CCVs (Fig. 5). This is equivalent to an AP-1:AP-2 ratio of 1.9:1. In brain, AP-1-positive CCVs represented 16.9% of the total leaving 83.1% accounted for by AP-2-positive CCVs. If the 1.9:1 ratio of AP-1:AP-2 is applied to brain, one would expect that 8.9% (16.9 divided by 1.9) of AP-2-positive CCVs in brain are involved in general endocytic housekeeping functions common to all tissues. The remaining 74.2% (83.1 minus 8.9) is thus anticipated to have a specialized function (Fig. 5). Comparing the CCVs that are derived from the plasma membrane (8.9% housekeeping and 74.2% specialized), we can calculate that 89% of the AP-2-positive CCVs are specialized for neuron-specific functions, most likely synaptic vesicle recycling.

Proteins Found and Novel Proteins—In total, 346 proteins

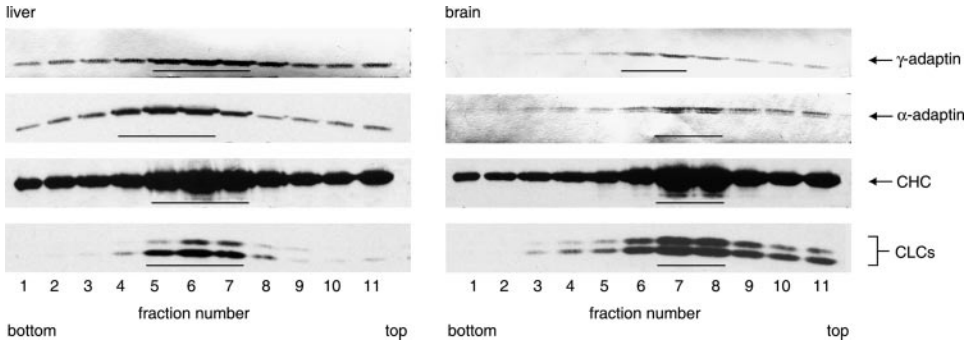

FIG. 3. **Differential migration profiles of CCV components.** CCVs from liver and brain were processed by velocity sedimentation analysis on linear sucrose gradients. Equal volume aliquots of the gradient, fractionated from the bottom, were processed for Western blot with AP-1 (γ-adaptin), AP-2 (α-adaptin), CHC, and CLC antibodies. The bands in which each antibody shows the strongest signal are indicated by the *black bar* underneath.

were reproducibly identified in the liver CCV preparations that were placed into 18 groups (supplemental table). Abundant Golgi proteins such as GM130, GRASP (Golgi peripheral membrane protein p65), or giantin, which are all found with high abundance in the Golgi proteome (26), were not detected in the CCV preparations. We did not detect abundant endoplasmic reticulum proteins such as calreticulin or ERp99 that Wu *et al.* (26) found in their Golgi proteome. Potential contaminants of the CCV preparations include abundant liver soluble enzymes and ribosomal proteins (supplemental table). Among the proteins identified, 21 are novel (Table I and supplemental table). We kept enthoprotin, NECAP 1, and FENS-1 (bold in Table I) in this group as they were referred to as novel when they were originally identified in the brain CCV proteome (18). Interestingly two of the novel proteins, RME-8 and Vac14, have been shown to be involved in endocytosis and vesicle trafficking in non-mammalian species (30–32). Two additional proteins can be associated with membrane trafficking by homology (70% identity to ADP-ribosylation factor (ARF)-like 6-interacting protein and EH domain-containing protein). None of the novel proteins were detected in brain CCVs with the exception of NECAP 1, enthoprotin, and FENS-1. This may reflect their involvement in more general, housekeeping clathrin-mediated trafficking at the plasma membrane or TGN.

DISCUSSION

The sequencing of animal genomes and the large scale sequencing of expressed genes coupled with advances in protein and peptide separation technologies and innovations in MS have led to an explosion in the use of proteomic approaches in biology. However, due to the complexity and dynamic range of protein expression, it is currently difficult to perform a satisfactory proteomic analysis of whole cells or tissues (33). Isolated organelles present an attractive target for proteomics as their protein complexity is reduced, and lower abundance proteins that are specific to the compartment are enriched relative to whole cell lysates (34–36). Numerous organelles and suborganellar compartments have now been analyzed by subcellular proteomics, and in almost all cases, novel proteins have been identified, and the global analysis of the organelle has provided insights into organelle function that may not have been possible from the analysis of a smaller subset of the proteins (34–36).

An important next step in subcellular proteomics is the development of approaches that allow for the quantitative comparison of organelle proteomes under different experimental paradigms. Several approaches have been tested so far for their relative quantitative nature. Among them are stable isotope labeling by amino acid in cell culture (SILAC) (37), DIGE (38), ICAT (39), absolute quantification (AQUA) (40), protein correlation profiling (41), protein abundance index (42), and peptide/spectral counts (18, 19). Although no extended comparative studies of all of these approaches have been performed, one can predict that each will have advantages and disadvantages and that their applicability will be influenced by the sample processing and MS apparatus available. The peptide accounting approach described here is extremely versatile and is applicable to the analysis of data generated from a wide variety of MS/MS configurations. Moreover the peptide accounting approach first analyzes the relative amounts of proteins within a sample and then compares the ratios between samples. This helps to alleviate changes due to differences in quantity and contamination of samples prepared at different time points and under different experimental conditions. In this study we applied the peptide counting approach in comparing the relative ratios of CHC and CLCs as well as APs from liver and brain CCVs and have further verified the results by Western blot.

One of the conclusions of our study is that the APs are expressed at lower levels than clathrin in different tissues and at both the TGN and the plasma membrane. Thus, it is likely that at all sites of clathrin-mediated membrane budding there is sufficient CHC to interact simultaneously with AP-1, AP-2, and a variety of other clathrin-binding partners even when each of these proteins utilize the same binding sites on the terminal domain of the CHC (43–45). As such, there is no need

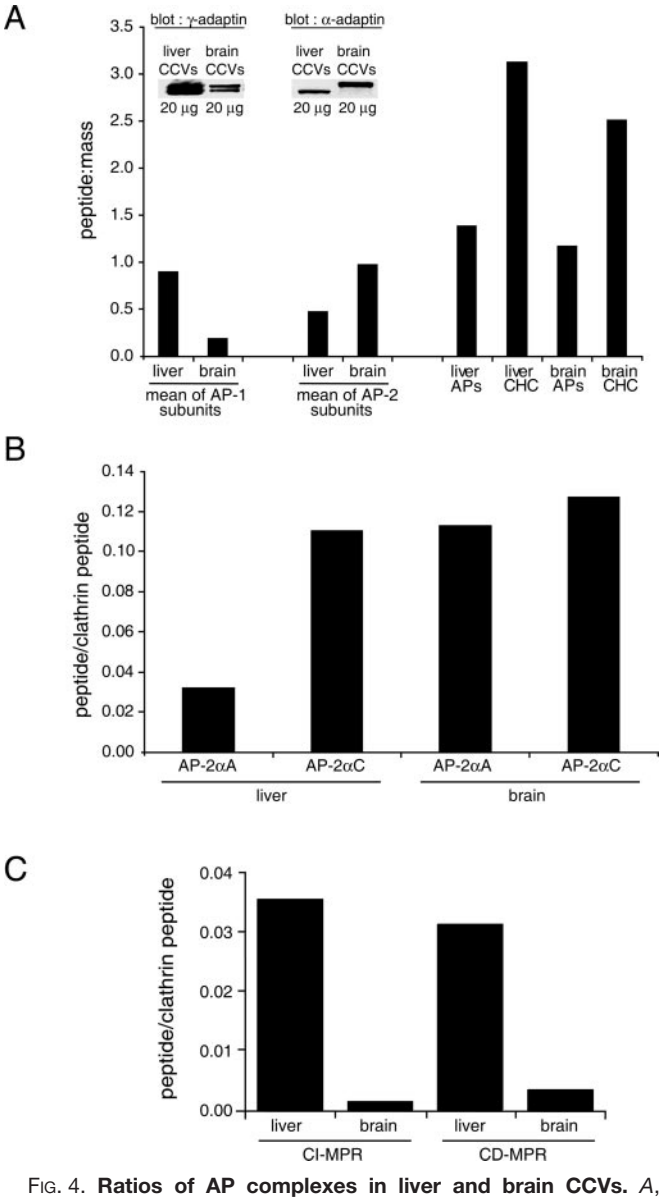

FIG. 4. **Ratios of AP complexes in liver and brain CCVs.** *A*, comparison of the total amount of normalized APs (mean of all four subunits) and CHC in brain and liver CCVs. For the *inset*, aliquots of liver and brain CCVs (20 μg for each) were processed for Western blot with antibodies against γ-adaptin and the αA isoform of α-adaptin. *B*, the total number of peptides for the αA and αC isoforms of α-adaptin from all three preparations of liver or brain CCVs, divided by the calculated mass of each protein, were apportioned to the total number of CHC peptides normalized for the molecular mass of the protein to yield a peptide/clathrin peptide index. *C*, the total number of peptides for the cation-independent (*CI-MPR*) and cation-dependent MPRs (*CD-MPR*) from all three preparations of liver or brain CCVs was used to calculate an MPR peptide to clathrin peptide index as described for the α-adaptin isoforms.

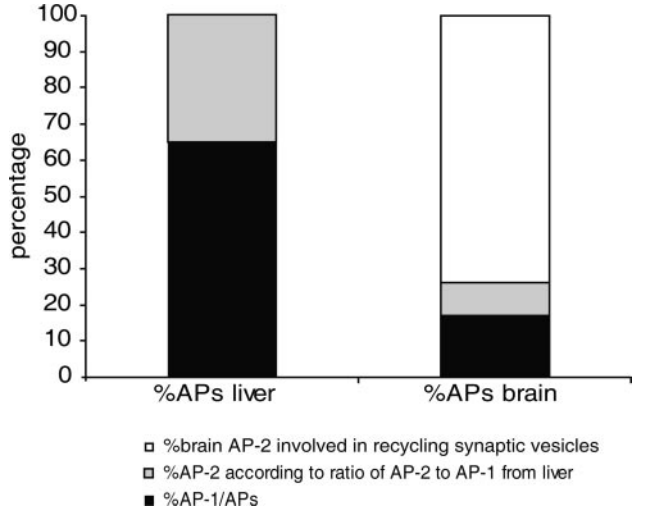

FIG. 5. **Percentage of AP-2-positive CCVs involved in synaptic vesicle recycling.** The *black section* of the *bars* represents the percentage of AP-1 relative to total APs found in liver and brain CCVs. The *gray section* in the *liver bar* represents the percentage of AP-2 relative to total APs in liver CCVs. The *gray section* in the *brain bar* represents the amount of AP-2 in brain that would be expected according to the ratio of AP-2 to AP-1 from liver. In *white* is the remaining AP-2, which is specialized for recycling synaptic vesicles. The percentages are based on the mean number of all four subunits for each adaptor from each tissue as for Fig. 4*B*.

for the sequential interaction of these proteins even when they interact with the CHC using the same motif. Thus, alternative cargo adaptors that bind to clathrin (43) could be found simultaneously in complexes with clathrin in a CCP that also utilizes classical APs. Another important finding of our study relates to the ratio of AP-1 and AP-2 in CCVs from brain and liver. The high ratio of AP-1 to AP-2 in liver CCVs is opposite to that found in brain, further emphasizing that the brain is specialized for endocytosis, likely due to the demand for synaptic vesicle recycling. We suggest that in brain, nine of 10 CCVs budding from the plasma membrane participate in the recycling of synaptic vesicles. Moreover from our calculations, we hypothesize that for a given number of CCVs the percentage that is involved in general housekeeping endocytosis in brain will be ~4-fold less than in liver (34.6% of total in liver, 8.9% of total in brain). Consistent with this idea, we were readily able to identify several endocytic cargo proteins in liver CCVs (supplemental table) that despite the fact they are known to be present in brain were not detected in brain CCVs. Examples include transferrin and transferrin receptor (46), mannose receptor C type 1 (47), low density lipoprotein related-protein (48), asialoglycoprotein and asialoglycoprotein receptor (49), hyaluronan receptor (50), and ferritin (51). In contrast, in brain we identified many of the known components of synaptic vesicles (18) in agreement with 74% of brain CCVs functioning in synaptic vesicles recycling. Thus, our quantitative organelle proteomic approach allowed us to determine the relative abundance of functionally specialized classes of CCVs within tissues.

It is generally thought that CHC and CLCs are obligate heterodimers with a 1:1 stoichiometry, and this has been demonstrated in brain (16–18). However, one study that may contradict this notion is from Liu *et al.* (52) who determined

that CLCs and the hub domain of CHC co-produced in bacteria do not form in a 1:1 ratio. Moreover loss of CLC in *Dictyostelium* has no effect on CHC steady state levels or triskelia formation (53), and knock-down of CLCs in non-neuronal mammalian cells does not affect clathrin-mediated endocytosis, further questioning an obligatory role for CLCs in CCV formation (54, 55). As determined by peptide counts and confirmed by Western blots, we have now demonstrated that there is a deficit of CLCs in CCVs from liver. Moreover this is likely to extend to all non-brain tissues and commonly used laboratory cell lines. The inability to detect CLCa fragments with the X16 antibody in microsome fractions shows that for all non-brain tissues and cell lines tested, with the exception of kidney, the deficit in CLCs relative to CHC cannot be simply explained by proteolytic degradation. Moreover the deficit in CLCs seen in crude cell lysates and the inability to detect the proteins in soluble fractions of any of the fractionation protocols utilized (data not shown) suggests that the deficit is likely due to the levels of CHC and CLCs stably expressed and is not due to a selective incorporation of CHC into CCVs. Previously Steven *et al.* (56) demonstrated a 1:1 stoichiometry between CHC and CLCs in liver CCVs. This ratio was determined by densitometric scanning of bands that were thought to correspond to CHC and CLCs in Coomassie Blue-stained CCV preparations. We detected CLC peptides from gel slices 16–21 containing bands assumed to correspond to CLCs (Supplemental Fig. 1), but we also detected peptides from other proteins identified in the proteomic analysis. In fact, CLCs represented ~12% of the peptides present in this region. Thus, it is not necessarily accurate to assign proteins to a specific band based on Coomassie Blue staining. However, proteomic analysis can provide a means to determine protein ratios within complex mixtures even in the face of heterogeneity within gel bands.

CLCs are clearly present and co-localized with CHC at CCPs at both the plasma membrane and the TGN (57, 58), and they are likely to function at both sites even if they function in a substoichiometric manner. One function for CLCs is to inhibit clathrin assembly (59), and assembly proteins are thus required to overcome this inhibition (60, 61). A lower ratio of CLCs to CHC may be necessary to ensure that assembly proteins alone are able to stimulate clathrin assembly in non-brain tissues. Because the ratio of CHC to CLCs in brain is 1:1, this would suggest that CCV formation in brain requires an additional level of regulation of CLCs. We demonstrated that the majority of brain CCVs function in synaptic vesicle recycling, and thus the additional level of CLC regulation may in fact be specific to synaptic vesicle endocytosis. Ca^{2+} is known to alleviate the inhibitory effect of CLCs on clathrin assembly *in vitro* (2, 62, 63). However, the physiological significance of this phenomenon has remained unclear given that CLCs bind to Ca^{2+} with a K_d of 25–50 μM (64). During synaptic vesicle exocytosis, there are bursts of Ca^{2+} at the active zone that can reach 100 μM or greater (65, 66). The bursts are local and transient, and Ca^{2+} concentrations decrease quickly around the active zone. Because the K_d for Ca^{2+} binding on CLCs is low, it would favor cage formation close to the active zone as proposed previously (67). The CCVs that begin to assemble close to the active zone will continue to mature as they move away from the active zone to finally pinch off at much lower Ca^{2+} concentrations (68). In this model, synaptic vesicle endocytosis requires assembly proteins working in conjunction with high Ca^{2+} concentrations. Consistent with this model, Sankaranarayanan and Ryan (69) have demonstrated that increases in intracellular Ca^{2+} concentration cause an acceleration of endocytosis of synaptic vesicles. In non-brain tissue where the Ca^{2+} concentration is low and yet the ratio of APs to CHC is similar, a decrease in the total amount of CLCs on triskelia could reduce the threshold for clathrin assembly.

Thus, through quantitative comparative proteomics, we are able to provide a model of the specialized role for CLCs in the regulation of synaptic vesicle endocytosis. Overall our study revealed new insights into the composition of coats and specializations of CCVs for trafficking.

Acknowledgments—We are particularly grateful to Frances M. Brodsky for discussions and for the generous gift of the X16 antibody. We thank Dr. Amanda Parmar, Pascal Lejeune, and Pierre-Emmanuel Foulon for help with ERACP, a multiple sequence comparison tool. We also thank all of the members of the laboratory, especially Valérie Legendre-Guillemin and Sébastien Thomas for discussions.

* This work was supported in part by Canadian Institutes of Health Research (CIHR) Grant MOP-15396 (to P. S. M.). Operating grants from the Genome Quebec/Genome Canada project Réseau Protéomique de Montréal, Montreal Proteomics Network financially supported this work. The costs of publication of this article were defrayed in part by the payment of page charges. This article must therefore be hereby marked "*advertisement*" in accordance with 18 U.S.C. Section 1734 solely to indicate this fact.

S The on-line version of this article (available at http://www.mcponline.org) contains supplemental material.

‡ Supported by a studentship from the CIHR.

§ A CIHR Investigator, a Killam Scholar, and a McGill University William Dawson Scholar. To whom correspondence may be addressed: Dept. of Neurology and Neurosurgery, Montreal Neurological Inst., McGill University, 3801 University St., Montreal, Québec H3A 2B4, Canada. E-mail: peter.mcpherson@mcgill.ca.

¶ To whom correspondence may be addressed: Dept. of Neurology and Neurosurgery, Montreal Neurological Inst., McGill University, 3801 University St., Montreal, Québec H3A 2B4, Canada. E-mail: francois.r.blondeau@mcgill.ca.

REFERENCES

1. McPherson, P. S., Kay, B. K., and Hussain, N. K. (2001) Signaling on the endocytic pathway. *Traffic* **2,** 375–384
2. Brodsky, F. M., Chen, C. Y., Knuehl, C., Towler, M. C., and Wakeham, D. E. (2001) Biological basket weaving: formation and function of clathrin-coated vesicles. *Annu. Rev. Cell Dev. Biol.* **17,** 517–568
3. Conner, S. D., and Schmid, S. L. (2003) Regulated portals of entry into the cell. *Nature* **422,** 37–44
4. Le Borgne, R., and Hoflack, B. (1998) Protein transport from the secretory to the endocytic pathway in mammalian cells. *Biochim. Biophys. Acta* **1404,** 195–209

5. Austin, C., Hinners, I., and Tooze, S. A. (2000) Direct and GTP-dependent interaction of ADP-ribosylation factor 1 with clathrin adaptor protein AP-1 on immature secretory granules. *J. Biol. Chem.* **275,** 21862–21869
6. Pearse, B. M., and Bretscher, M. S. (1981) Membrane recycling by coated vesicles. *Annu. Rev. Biochem.* **50,** 85–101
7. Sudhof, T. C. (2004) The synaptic vesicle cycle. *Annu. Rev. Neurosci.* **27,** 509–547
8. Murthy, V. N., and De Camilli, P. (2003) Cell biology of the presynaptic terminal. *Annu. Rev. Neurosci.* **26,** 701–728
9. Bauerfeind, R., David, C., Grabs, D., McPherson, P. S., Nemoto, Y., Slepnev, V. I., Takei, K., and De Camilli, P. (1998) Recycling of synaptic vesicles. *Adv. Pharmacol.* **42,** 253–257
10. Bauerfeind, R., David, C., Galli, T., McPherson, P. S., Takei, K., and De Camilli, P. (1995) Molecular mechanisms in synaptic vesicle endocytosis. *Cold Spring Harb. Symp. Quant. Biol.* **60,** 397–404
11. Boehm, M., and Bonifacino, J. S. (2001) Adaptins: the final recount. *Mol. Biol. Cell* **12,** 2907–2920
12. Ball, C. L., Hunt, S. P., and Robinson, M. S. (1995) Expression and localization of α-adaptin isoforms. *J. Cell Sci.* **108,** 2865–2875
13. Ritter, B., and McPherson, P. S. (2004) Molecular mechanisms in clathrin-mediated membrane budding, in *Topics in Current Genetics: Regulatory Mechanisms of Intracellular Membrane Transport* (Keranen, S., and Jantti, J., eds) Vol. 10, pp. 9–37, Springer-Verlag, Berlin
14. Lindner, R., and Ungewickell, E. (1992) Clathrin-associated proteins of bovine brain coated vesicles. An analysis of their number and assembly-promoting activity. *J. Biol. Chem.* **267,** 16567–16573
15. Wasiak, S., Legendre-Guillemin, V., Puertollano, R., Blondeau, F., Girard, M., de Heuvel, E., Boismenu, D., Bell, A. W., Bonifacino, J. S., and McPherson, P. S. (2002) Enthoprotin: a novel clathrin-associated protein identified through subcellular proteomics. *J. Cell Biol.* **158,** 855–862
16. Ungewickell, E., and Branton, D. (1981) Assembly units of clathrin coats. *Nature* **289,** 420–422
17. Kirchhausen, T., and Harrison, S. C. (1981) Protein organization in clathrin trimers. *Cell* **23,** 755–761
18. Blondeau, F., Ritter, B., Allaire, P. D., Wasiak, S., Girard, M., Hussain, N. K., Angers, A., Legendre-Guillemin, V., Roy, L., Boismenu, D., Kearney, R. E., Bell, A. W., Bergeron, J. J., and McPherson, P. S. (2004) Tandem MS analysis of brain clathrin-coated vesicles reveals their critical involvement in synaptic vesicle recycling. *Proc. Natl. Acad. Sci. U. S. A.* **101,** 3833–3838
19. Liu, H., Sadygov, R. G., and Yates, J. R., III (2004) A model for random sampling and estimation of relative protein abundance in shotgun proteomics. *Anal. Chem.* **76,** 4193–4201
20. Brodsky, F. M. (1985) Clathrin structure characterized with monoclonal antibodies. II. Identification of in vivo forms of clathrin. *J. Cell Biol.* **101,** 2055–2062
21. Pilch, P. F., Shia, M. A., Benson, R. J., and Fine, R. E. (1983) Coated vesicles participate in the receptor-mediated endocytosis of insulin. *J. Cell Biol.* **96,** 133–138
22. Girard, M., Allaire, P. D., Blondeau, F., and McPherson, P. S. (2004) Isolation of clathrin-coated vesicles by differential and density gradient centrifugation, in *Current Protocols in Cell Biology* (Bonifacino, J., Lippincott-Schwartz, J., Dasso, M., Harford, J., and Yamada, K., eds) pp. 3.13.1–3.13.20, John Wiley and Sons, Inc., New York
23. Baudhuin, P., Evrard, P., and Berthet, J. (1967) Electron microscopic examination of subcellular fractions. I. The preparation of representative samples from suspensions of particles. *J. Cell Biol.* **32,** 181–191
24. Simionescu, N., and Simionescu, M. (1976) Galloylglucoses of low molecular weight as mordant in electron microscopy. II. The moiety and functional groups possibly involved in the mordanting effect. *J. Cell Biol.* **70,** 622–633
25. Perkins, D. N., Pappin, D. J., Creasy, D. M., and Cottrell, J. S. (1999) Probability-based protein identification by searching sequence databases using mass spectrometry data. *Electrophoresis* **20,** 3551–3567
26. Wu, C. C., MacCoss, M. J., Mardones, G., Finnigan, C., Mogelsvang, S., Yates, J. R., III, and Howell, K. E. (2004) Organellar proteomics reveals Golgi arginine dimethylation. *Mol. Biol. Cell* **15,** 2907–2919
27. Jackson, A. P., and Parham, P. (1988) Structure of human clathrin light chains. Conservation of light chain polymorphism in three mammalian species. *J. Biol. Chem.* **263,** 16688–16695
28. Wong, D. H., Ignatius, M. J., Parosky, G., Parham, P., Trojanowski, J. Q., and Brodsky, F. M. (1990) Neuron-specific expression of high-molecular-weight clathrin light chain. *J. Neurosci.* **10,** 3025–3031
29. Maycox, P. R., Link, E., Reetz, A., Morris, S. A., and Jahn, R. (1992) Clathrin-coated vesicles in nervous tissue are involved primarily in synaptic vesicle recycling. *J. Cell Biol.* **118,** 1379–1388
30. Chang, H. C., Hull, M., and Mellman, I. (2004) The J-domain protein Rme-8 interacts with Hsc70 to control clathrin-dependent endocytosis in *Drosophila*. *J. Cell Biol.* **164,** 1055–1064
31. Zhang, Y., Grant, B., and Hirsh, D. (2001) RME-8, a conserved J-domain protein, is required for endocytosis in Caenorhabditis elegans. *Mol. Biol. Cell* **12,** 2011–2021
32. Dove, S. K., McEwen, R. K., Mayes, A., Hughes, D. C., Beggs, J. D., and Michell, R. H. (2002) Vac14 controls PtdIns(3,5)P(2) synthesis and Fab1-dependent protein trafficking to the multivesicular body. *Curr. Biol.* **12,** 885–893
33. Huber, L. A. (2003) Is proteomics heading in the wrong direction? *Nat. Rev. Mol. Cell. Biol.* **4,** 74–80
34. Taylor, S. W., Fahy, E., and Ghosh, S. S. (2003) Global organellar proteomics. *Trends Biotechnol.* **21,** 82–88
35. Brunet, S., Thibault, P., Gagnon, E., Kearney, P., Bergeron, J. J., and Desjardins, M. (2003) Organelle proteomics: looking at less to see more. *Trends Cell Biol.* **13,** 629–638
36. Ritter, B., Blondeau, F., Denisov, A. Y., Gehring, K., and McPherson, P. S. (2004) Molecular mechanisms in clathrin-mediated membrane budding revealed through subcellular proteomics. *Biochem. Soc. Trans.* **32,** 769–773
37. de Hoog, C. L., Foster, L. J., and Mann, M. (2004) RNA and RNA binding proteins participate in early stages of cell spreading through spreading initiation centers. *Cell* **117,** 649–662
38. Ornstein, D. K., and Petricoin, E. F., III (2004) Proteomics to diagnose human tumors and provide prognostic information. *Oncology* **18,** 521–529
39. MacCoss, M. J., Wu, C. C., Liu, H., Sadygov, R., and Yates, J. R., III (2003) A correlation algorithm for the automated quantitative analysis of shotgun proteomics data. *Anal. Chem.* **75,** 6912–6921
40. Gerber, S. A., Rush, J., Stemman, O., Kirschner, M. W., and Gygi, S. P. (2003) Absolute quantification of proteins and phosphoproteins from cell lysates by tandem MS. *Proc. Natl. Acad. Sci. U. S. A.* **100,** 6940–6945
41. Andersen, J. S., Wilkinson, C. J., Mayor, T., Mortensen, P., Nigg, E. A., and Mann, M. (2003) Proteomic characterization of the human centrosome by protein correlation profiling. *Nature* **426,** 570–574
42. Rappsilber, J., Ryder, U., Lamond, A. I., and Mann, M. (2002) Large-scale proteomic analysis of the human spliceosome. *Genome Res.* **12,** 1231–1245
43. Traub, L. M. (2003) Sorting it out: AP-2 and alternate clathrin adaptors in endocytic cargo selection. *J. Cell Biol.* **163,** 203–208
44. Ritter, B., Denisov, A. Y., Philie, J., Deprez, C., Tung, E. C., Gehring, K., and McPherson, P. S. (2004) Two WXXF-based motifs in NECAPs define the specificity of accessory protein binding to AP-1 and AP-2. *EMBO J.* **23,** 3701–3710
45. Miele, A. E., Watson, P. J., Evans, P. R., Traub, L. M., and Owen, D. J. (2004) Two distinct interaction motifs in amphiphysin bind two independent sites on the clathrin terminal domain β-propeller. *Nat. Struct. Mol. Biol.* **11,** 242–248
46. Pearse, B. M. (1982) Coated vesicles from human placenta carry ferritin, transferrin, and immunoglobulin G. *Proc. Natl. Acad. Sci. U. S. A.* **79,** 451–455
47. Harris, N., Super, M., Rits, M., Chang, G., and Ezekowitz, R. A. (1992) Characterization of the murine macrophage mannose receptor: demonstration that the downregulation of receptor expression mediated by interferon-γ occurs at the level of transcription. *Blood* **80,** 2363–2373
48. Orr, A. W., Pedraza, C. E., Pallero, M. A., Elzie, C. A., Goicoechea, S., Strickland, D. K., and Murphy-Ullrich, J. E. (2003) Low density lipoprotein receptor-related protein is a calreticulin coreceptor that signals focal adhesion disassembly. *J. Cell Biol.* **161,** 1179–1189
49. Ciechanover, A., Schwartz, A. L., and Lodish, H. F. (1983) Sorting and recycling of cell surface receptors and endocytosed ligands: the asialoglycoprotein and transferrin receptors. *J. Cell. Biochem.* **23,** 107–130
50. Weigel, J. A., and Weigel, P. H. (2003) Characterization of the recombinant rat 175-kDa hyaluronan receptor for endocytosis (HARE). *J. Biol. Chem.* **278,** 42802–42811

51. Hulet, S. W., Heyliger, S. O., Powers, S., and Connor, J. R. (2000) Oligodendrocyte progenitor cells internalize ferritin via clathrin-dependent receptor mediated endocytosis. *J. Neurosci. Res.* **61,** 52–60
52. Liu, S. H., Wong, M. L., Craik, C. S., and Brodsky, F. M. (1995) Regulation of clathrin assembly and trimerization defined using recombinant triskelion hubs. *Cell* **83,** 257–267
53. Wang, J., Virta, V. C., Riddelle-Spencer, K., and O'Halloran, T. J. (2003) Compromise of clathrin function and membrane association by clathrin light chain deletion. *Traffic* **4,** 891–901
54. Huang, F., Khvorova, A., Marshall, W., and Sorkin, A. (2004) Analysis of clathrin-mediated endocytosis of epidermal growth factor receptor by RNA interference. *J. Biol. Chem.* **279,** 16657–16661
55. Yang, D., Buchholz, F., Huang, Z., Goga, A., Chen, C. Y., Brodsky, F. M., and Bishop, J. M. (2002) Short RNA duplexes produced by hydrolysis with Escherichia coli RNase III mediate effective RNA interference in mammalian cells. *Proc. Natl. Acad. Sci. U. S. A.* **99,** 9942–9947
56. Steven, A. C., Hainfeld, J. F., Wall, J. S., and Steer, C. J. (1983) Mass distributions of coated vesicles isolated from liver and brain: analysis by scanning transmission electron microscopy. *J. Cell Biol.* **97,** 1714–1723
57. Gaidarov, I., Santini, F., Warren, R. A., and Keen, J. H. (1999) Spatial control of coated-pit dynamics in living cells. *Nat. Cell Biol.* **1,** 1–7
58. Ehrlich, M., Boll, W., Van Oijen, A., Hariharan, R., Chandran, K., Nibert, M. L., and Kirchhausen, T. (2004) Endocytosis by random initiation and stabilization of clathrin-coated pits. *Cell* **118,** 591–605
59. Ungewickell, E., and Ungewickell, H. (1991) Bovine brain clathrin light chains impede heavy chain assembly *in vitro*. *J. Biol. Chem.* **266,** 12710–12714
60. Legendre-Guillemin, V., Metzler, M., Lemaire, J. F., Philie, J., Gan, L., Hayden, M. R., and McPherson, P. S. (2004) HIP1 (huntingtin interacting protein 1) regulates clathrin assembly through direct binding to the regulatory region of the clathrin light chain. *J. Biol. Chem.* **280,** 6101–6108
61. Chen, C. Y., and Brodsky, F. M. (2004) Huntingtin-interacting protein 1 (Hip1) and Hip1-related protein (Hip1R) bind the conserved sequences of clathrin light chains and thereby influence clathrin assembly *in vitro* and actin distribution *in vivo*. *J. Biol. Chem.* **280,** 6109–6117
62. Keen, J. H., Willingham, M. C., and Pastan, I. H. (1979) Clathrin-coated vesicles: isolation, dissociation and factor-dependent reassociation of clathrin baskets. *Cell* **16,** 303–312
63. Brodsky, F. M., Hill, B. L., Acton, S. L., Nathke, I., Wong, D. H., Ponnambalam, S., and Parham, P. (1991) Clathrin light chains: arrays of protein motifs that regulate coated-vesicle dynamics. *Trends Biochem. Sci.* **16,** 208–213
64. Mooibroek, M. J., Michiel, D. F., and Wang, J. H. (1987) Clathrin light chains are calcium-binding proteins. *J. Biol. Chem.* **262,** 25–28
65. Matthews, G. (1996) Neurotransmitter release. *Annu. Rev. Neurosci.* **19,** 219–233
66. Augustine, G. J., Santamaria, F., and Tanaka, K. (2003) Local calcium signaling in neurons. *Neuron* **40,** 331–346
67. Heuser, J. E., and Reese, T. S. (1973) Evidence for recycling of synaptic vesicle membrane during transmitter release at the frog neuromuscular junction. *J. Cell Biol.* **57,** 315–344
68. Cousin, M. A., and Robinson, P. J. (2000) Ca^{2+} influx inhibits dynamin and arrests synaptic vesicle endocytosis at the active zone. *J. Neurosci.* **20,** 949–957
69. Sankaranarayanan, S., and Ryan, T. A. (2001) Calcium accelerates endocytosis of vSNAREs at hippocampal synapses. *Nat. Neurosci.* **4,** 129–136